

Original Article

Effects of PDTC on NF- κ B expression and apoptosis in rats with severe acute pancreatitis-associated lung injury

Shihai Kan¹, Hongying Zhou¹, Changzhu Jin², Huijun Yang¹

¹Department of Human Anatomy, West China School of Preclinical and Forensic Medicine, Sichuan University, No. 17 Renmin South Road, Chengdu 610041, China; ²Department of Human Anatomy, Binzhou Medical College, No. 346 Guanhai Road, Yantai 264003, China

Received October 27, 2014; Accepted March 2, 2015; Epub March 15, 2015; Published March 30, 2015

Abstract: We investigated the effects of pyrrolidine dithiocarbamate (PDTC) on intrapulmonary expression of nuclear factor- κ B (NF- κ B), and apoptosis in rats with severe acute pancreatitis (SAP). We induced SAP, then used immunohistochemistry, TUNEL staining, quantitative PCR assays and western blotting to examine PDTC effects. Treatment with PDTC resulted in interstitial edema and widening of the basement membrane, with swollen mitochondria and aggregation of nuclear chromatin. Expression of NF- κ B, Fas, Bcl-2 and TNF- α in lung tissues of SAP rats was increased, with NF- κ B, Fas and TNF- α levels maximal after 6 h. PDTC appeared to ameliorate pathological changes, with low levels of NF- κ B, Fas, TNF- α , and Caspase-3 mRNA observed and a lower apoptosis index compared with that seen in SAP rats. Expression of NF- κ B could be involved in lung tissue apoptosis during SAP. We postulate that PDTC inhibits the activation of NF- κ B and apoptosis, effectively alleviating the severity of lung injury.

Keywords: NF- κ B, Caspase-3, apoptosis, severe acute pancreatitis, lung injury

Introduction

Severe acute pancreatitis (SAP) is characterized by dangerous onset, rapid progression and involvement, multiple complications, high morbidity and high mortality. Mortality can approach 50% [1] because of the induction of a systemic inflammatory response syndrome (SIRS) during the early stages of the disease, subsequently leading to multiple organ dysfunction (MODS) [2]. Acute lung injury is common, with approximately 20% of these patients developing acute respiratory distress syndrome (ARDS). ARDS is a primary cause of patient death during the early stages of SAP [3]. The precise pathogenesis of severe pancreatitis-associated lung injury is yet to be fully elucidated, but it was recently found that nuclear factor (NF)- κ B plays a critical role in the initiation of SAP. Its activation is believed to be an important early event in acute pancreatitis [4]. There is evidence that NF- κ B plays a key role in the control of cytokine-induced expression of genes related to inflammatory immune

responses [5]. NF- κ B can regulate the transcription of inflammatory factors, which leads to local inflammation in multiple systems and/or organs. In a previous study we showed that expression of NF- κ B induced iNOS mRNA expression in rat SAP models, which resulted in the generation of excess nitric oxide (NO), thereby exacerbating lung injury [6]. Pyrrolidine dithiocarbamate (PDTC), a selective NF- κ B inhibitor and antioxidant, can inhibit the activation of NF- κ B in many cell types [7].

Recent studies have revealed that NF- κ B can promote or inhibit apoptosis by regulating apoptosis-related genes [8, 9]. The anti-apoptosis pathway involving NF- κ B is associated with genes encoding cytokines and whose functions include "death receptors" and apoptotic regulation [10-12]. Activation of NF- κ B has a dual role in apoptosis and could be the set point of cell survival and apoptosis. Apoptosis-inducing genes include p53, Fas, ICE, rpr, Bcl-xs, Bax, Bak, Bad, bid, and bik. Genes that inhibit apoptosis include Bcl-2, the IAP family, Bcl-xl, AI, Bcl-

w, Mcl, and BAG-1 [13, 14]. The signal transduction mechanisms of apoptosis are very complex, involving at least three pathways (mitochondrial, death receptor, and endoplasmic reticulum pathways) [21]. Fas and TNF- α are important regulatory proteins of the exogenous death receptor pathway, while Bcl-2 is involved in the transduction of the intrinsic mitochondria pathway [15]. The cascade of apoptosis signals in the aforementioned pathways causes cysteine protease family (Caspase) activation. Caspase-3, the key executor of apoptosis, forms a central link in the process of apoptosis signal transduction, with determination of Caspase-3 levels reflecting the level of cellular apoptosis [16].

In this study, we generated models of rat SAP using Aho's improved method [17] and then investigated the effects of NF- κ B activation and cell apoptosis over the course of severe pancreatitis-associated lung injury. We also assessed the effects of PDTC on SAP pathology.

Materials and methods

Reagents

We purchased polyclonal antibodies against NF- κ B P65, Fas, Bcl-2 and TNF- α and a monoclonal antibody against Caspase-3 from the Wuhan Boster Biotechnology Company (Wuhan, China). The immunohistochemistry kit was provided by the Beijing Zhongshang Biotechnology Company (Beijing, China). We purchased an apoptosis detection kit from Roche Diagnostics. SYBR MIX (QPK-201) was purchased from TOYOBO (Japan). The 5**Taq* MIX was purchased from uBio (USA). Primer synthesis and probe modifications were conducted by the Biotechnology Limited Company of Shanghai (China). Sodium taurocholate and PDTC were from Sigma (USA). The western blot system was purchased from Amersham Pharmacia Biotech (USA).

Animal experiments

Our animal study was approved by the Institutional Animal Care and Use Committee of Sichuan University. Healthy male Sprague-Dawley rats weighing 250-300 g were provided by the Experimental Animal Center of Binzhou Medical College. Animals were randomly divid-

ed into three groups ($n = 20$ rats per group): the SAP group; the PDTC group; and the control (sham operation) group. Rats were kept at 23°C on a 12-h light/dark cycle and allowed free access to water and standard laboratory chow. At 12 h prior to the start of experiments, animals were deprived of food but allowed access to water. Rats were anesthetized by intraperitoneal injection of 1% pentobarbital sodium (0.3 ml/100 g body weight) and operations were performed under aseptic conditions. We induced SAP in rats of the appropriate group according to the method of Aho et al [16]. Rats in the PDTC group were administered PDTC (100 mg/kg body weight) into the peritoneal cavity prior to the induction of SAP. Rats in the control group underwent a sham operation where nothing was infused. The pancreas was flipped and gently struck three times. Rats from all groups were subcutaneously injected with 5 ml of normal saline into their backs. Once rats had recovered from the anesthetic, they were allowed access to water.

Sample collection and storage

Rats were killed by an overdose of pentobarbital sodium at 3, 6, 12, and 24 h after the operation and blood was collected by cardiac puncture. Blood samples were incubated at 37°C for 10 min and centrifuged (10 min, 3000 \times g). Supernatants were aliquoted into sterilized 1.5-ml microcentrifuge tubes (Eppendorf) and stored at -20°C for later use. A portion of lung and pancreas tissue from each rat was removed and placed in liquid nitrogen overnight, then stored at -80°C until required. Separate portions of lung and pancreas tissue from each rat were fixed by immersion in 4% paraformaldehyde, embedded in paraffin wax and sectioned (4- μ m thickness). Small pieces of lung tissue were treated with 3% glutaraldehyde, fixed at 4°C and subjected to electron microscopy.

Serum amylase and lipase levels

An Olympus AU5400 fully automatic biochemical analyzer (Olympus Corp., Tokyo, Japan) was used to determine plasma amylase and lipase levels.

Histopathological examination

Changes in pancreas and lung tissues were observed macroscopically and microscopically.

Effects of PDTC on NF- κ B and apoptosis

Tissue sections (4- μ m thickness) were deparaffinized and stained with hematoxylin and eosin (HE) for histopathological examination.

Transmission electron microscopy (TEM)

Lung tissue fixed with glutaraldehyde was rinsed with 0.2 M phosphate-buffered saline (PBS; pH 7.4) and incubated in 1% osmium tetroxide at 4°C for 2 h. Tissues were then dehydrated through a graded acetone series: 50% acetone (4°C, 15 min); 70% acetone and 2% uranyl acetate (4°C, overnight); 90% acetone (4°C, 10 min); and 100% acetone (4°C, 5 min). After dehydration, samples were infiltrated with epoxy resin and epoxy propane at a ratio of 1:1 for 1 h at 4°C. Samples were embedded in resin and ultrastructural changes inspected and photographed with a transmission electron microscope (JEOL-1400; Jeol, Japan).

Terminal dUTP nick-end labeling (TUNEL) staining

TUNEL staining was performed on paraffin-embedded sections using an *in situ* cell death detection kit (Roche) according to the manufacturer's instructions. Five sections were randomly selected from each group and five fields of view (400 \times magnification) for each section were randomly examined and cells counted by a single blinded observer in a coded randomized order. Results were presented as the apoptosis index (AI), the ratio of TUNEL-positive cells to total cells in the same field of view.

Immunohistochemical staining

The S-P method was used to detect expression of NF- κ B P65, Fas, Bcl-2 and TNF- α proteins in lung tissue. Fixed sections were incubated with the appropriate primary and secondary antibodies. Color reactions were developed using diaminobenzidine (DAB) solution according to the manufacturer's instructions. PBS was used as a negative control in place of an antibody. For semi-quantitative analyses, areas of positive staining were defined by two independent investigators using Image-Pro 6.0 Plus (Media Cybernetics). Five fields of view for each section were randomly selected, images acquired, and integrated optical density (IOD) determined [density (mean) = IOD/area].

Caspase-3 mRNA expression levels

Total RNA from lung tissues was extracted with Trizol reagent. Following reverse-transcription, conventional PCR using the specific primer pairs rCaspase-3 (5'-TGG AAT TGA TGG ATA GTG-3' and 5'-CCT GAA TGA TGA AGA GTT-3') and β -actin (5'-ATG TGG ATC AGC AAG CAG GA-3' and 5'-AAG GGT GTA AAA CGC AGC TCA-3') were conducted. Each reaction contained 10 μ l of SYBR Green Supermix, 0.5 μ l of each primer, 0.8 μ l of cDNA template, and 8.2 μ l of DEPC-treated water. Thermal cycling conditions involved a 50°C incubation for 2 min, then a denaturation step at 95°C for 10 min, followed by 40 amplification cycles (20 s at 95°C, and 60 s at 60°C) on an ABI7500 thermal cycler. We used β -actin as an internal reference gene. All samples were tested three times. Fluctuations in the fluorescent signal were continuously detected. The threshold cycle (Ct value) was recorded when the signal intensity reached a certain level. We analyzed the expression data for Caspase-3 mRNA using the $2^{-\Delta\Delta Ct}$ method [18].

Caspase-3 western blotting

Approximately 0.1 g of lung tissue that had been placed in liquid nitrogen was washed three times with cold PBS. Tissue was then homogenized and resuspended in ice-cold solubilization buffer (50 mM Tris-HCl pH 8, 150 mM NaCl, 0.1% SDS, 100 μ g/ml phenylmethylsulfonyl fluoride) supplemented with protease inhibitors (Sigma). Proteins were extracted from tissues using ultrasonication and their concentration determined with a NanoDrop 2000 spectrophotometer (Thermo Scientific, USA). Proteins were separated by sodium dodecyl sulfate polyacrylamide gel electrophoresis (SDS-PAGE) and then transferred onto polyvinylidene difluoride (PVDF) membranes (Millipore). After blocking with 5% (w/v) skim milk in Tris-buffered saline supplemented with Tween 20 (TBST) for 1 h at room temperature, membranes were incubated with a mouse monoclonal antibody against Caspase-3 (1:300 dilution) overnight at 4°C. Membranes were washed three times with TBST (10 min each wash) and then incubated with a horseradish peroxidase (HRP)-conjugated goat anti-rabbit secondary antibody (1:3000) for 1 h at room temperature. Membranes were washed three times with TBST (10

Effects of PDTC on NF- κ B and apoptosis

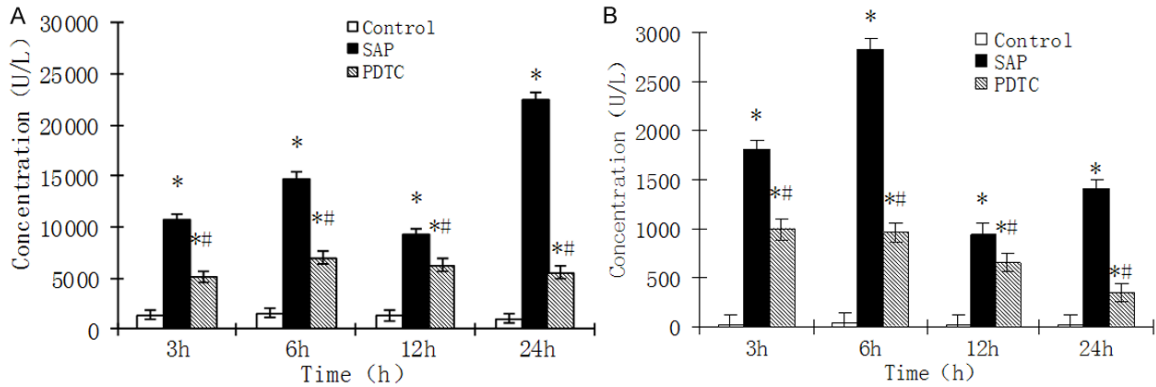


Figure 1. A. Serum amylase levels at various time points for rat groups. * $P < 0.05$, SAP group vs. control group; # $P < 0.05$, PDTC group vs. SAP group. Values are expressed as mean \pm SD. B. Serum lipase levels at various time points for rat groups. * $P < 0.05$, SAP group vs. control group; # $P < 0.05$, PDTC group vs. SAP group. Values are expressed as mean \pm SD.

min each wash) and specific Caspase-3 bands detected using enhanced chemiluminescence (ECL). The optical density of each band was measured using Image-Pro 6.0 Plus, with β -Actin used as an internal loading control.

Statistical analysis

Values are presented as the mean \pm standard deviation (SD). Our data were analyzed with Student's t test and one-way analysis of variance (ANOVA) with the Newman-Keuls post hoc test using SPSS 13.0 (SPSS Inc., USA). Correlations were tested using the Spearman rank correlation coefficient. A P -value of 0.05 or less was considered statistically significant.

Results

Serum amylase and lipase

Serum amylase levels in the SAP and PDTC rats were significantly higher than those in control rats at all time points ($P < 0.01$). Serum amylase levels in PDTC rats were significantly lower than those in the SAP groups ($P < 0.05$; **Figure 1A**). Changes in serum lipase levels were similar to those seen for serum amylase levels. Serum lipase levels in SAP and PDTC rats were significantly higher than in control rats at various time points ($P < 0.01$). For PDTC rats, lipase levels were significantly lower than for SAP rats ($P < 0.05$) except at 12 h ($P > 0.05$; **Figure 1B**). After establishment of the SAP model, the serum amylase and lipase levels changed with time, peaking at 6 h and remaining high up to 24 h.

Pathological observations

Hyperemia, edema, necrosis of the pancreas, and bloody ascites could be seen in each SAP rat. A few calcic spots were noticed on the mesentery and greater omentum. Ascitic fluids and calcic spots were significantly decreased in PDTC-treated rats. No changes were observed in control group rats. Pulmonary edema, petechiae scattered on the surface of lung, and a small amount of fluid had accumulated in the thoracic cavity of rats in the SAP group. Pulmonary local brown areas of atelectasis were seen at 6, 12, and 24 h. These changes were less obvious in the PDTC-treated rats. No obvious changes were observed in rats of the control group.

The pancreas tissue was normal in most rats of the control group. Focal edema and infiltration of a small number of inflammatory cells were seen in the pancreas of a few rats (**Figure 2A**). Inflammatory and erythrocyte cells were observed in the interstitial space of the pancreas for all rats in the SAP group. Severe swelling and necrosis of pancreatic acinar cells was seen; the range of pancreatic lobule necrosis was increased over time and spread to the whole pancreatic lobule (**Figure 2B-D**). The pathologic changes in rats of the PDTC group were similar to those seen in rats of the SAP group. Exudates, hemorrhaging and infiltration of inflammatory cells were significantly lower than those in the SAP group. No obvious changes were observed in the lung tissue of rats in the control group (**Figure 2E**). Significant changes were observed in the lungs of rats in the SAP

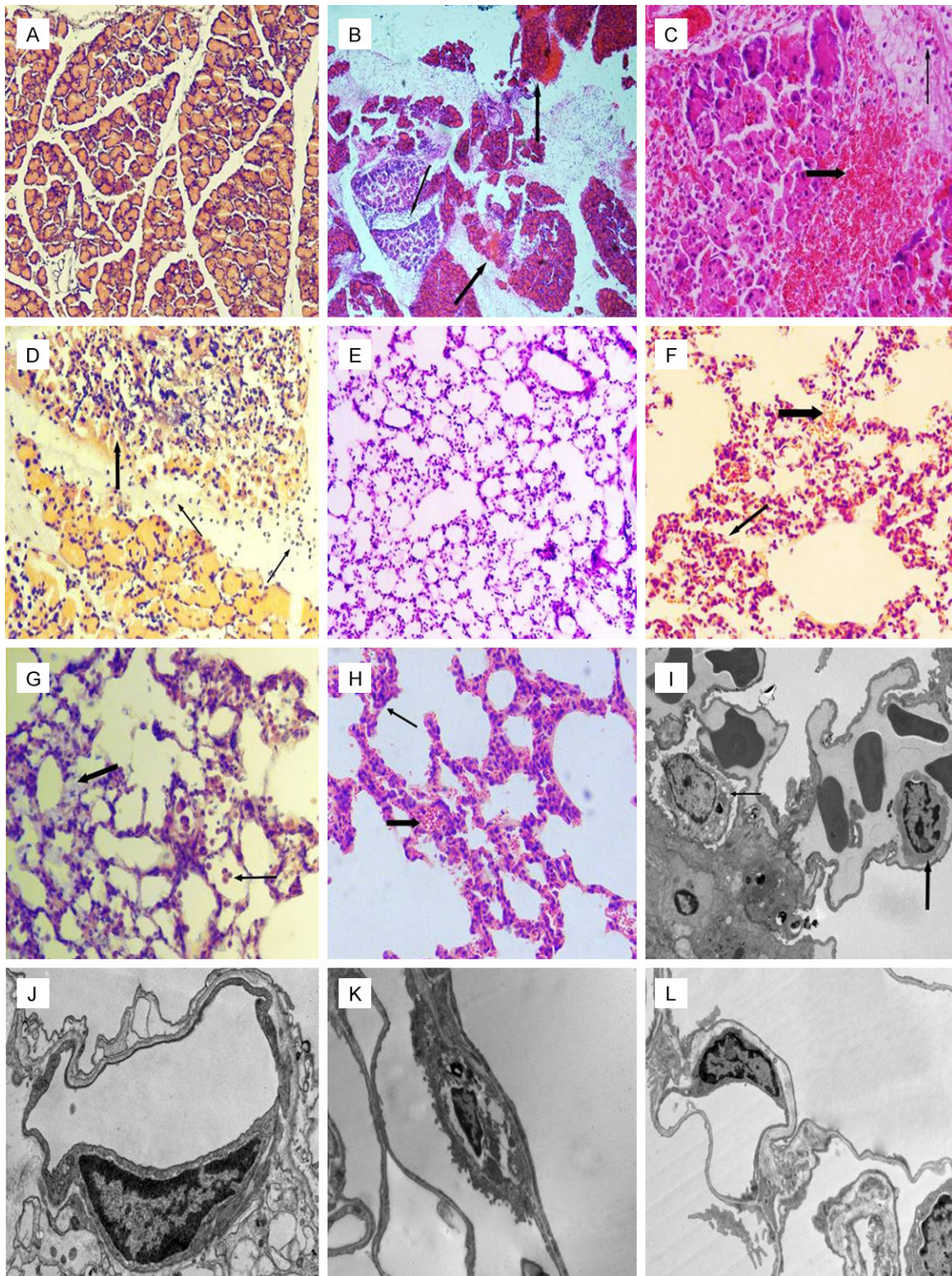


Figure 2. A. HE staining of pancreas tissue from the control group ($\times 100$ magnification). B. HE staining of pancreas tissue from the SAP 12 h group. Necrosis of pancreatic lobules and exudation of erythrocytes (thick arrow) is seen. Infiltration of inflammatory cells into the interstitium (thin arrow) was also observed ($\times 100$ magnification). C. HE staining of pancreas tissue from the PDTC 12 h group. Erythrocyte exudation (thick arrow) and inflammatory cell infiltration (thin arrow) in the interstitium of pancreas was observed ($\times 200$ magnification). D. HE staining of pancreas tissue from the SAP 12 h group. Local necrosis of pancreatic lobules with exudation of erythrocytes (thick

Effects of PDTC on NF-κB and apoptosis

arrow) and infiltration of inflammatory cells in the interstitium (thin arrow) were seen ($\times 200$ magnification). E. HE staining of pulmonary tissue from the control group ($\times 100$ magnification). F. HE staining of lung tissue from the SAP 12 h group. Infiltration of inflammatory cells and erythrocyte exudation (thick arrow), atelectasis of local lobule and anomalies in the structure (thin arrow) can be seen ($\times 200$ magnification). G. HE staining of lung tissue from the SAP 6 h group. Infiltration of inflammatory cells (thick arrow) and interstitial edema (thin arrow) was observed ($\times 200$ magnification). H. HE staining of lung tissue from the PDTC 12 h group. Infiltration of inflammatory cells (thick arrow), atelectasis and alveolar collapse (thin arrow) can be seen ($\times 200$ magnification). I. Electron micrograph of lung tissue from the control group. Type II alveolar epithelial cells (thin arrow). Microvascular endothelial cells (thick arrow) ($\times 50,000$ magnification). J. Electron micrograph of lung tissue from the SAP 6 h group highlighting microvascular endothelial cells ($\times 20,000$ magnification). K. Electron micrograph of lung tissue from the SAP 12 h group showing type II alveolar epithelial cells ($\times 5000$ magnification). L. Electron micrograph of lung tissue from the PDTC 6 h group showing a microvascular endothelial cell ($\times 8000$ magnification).

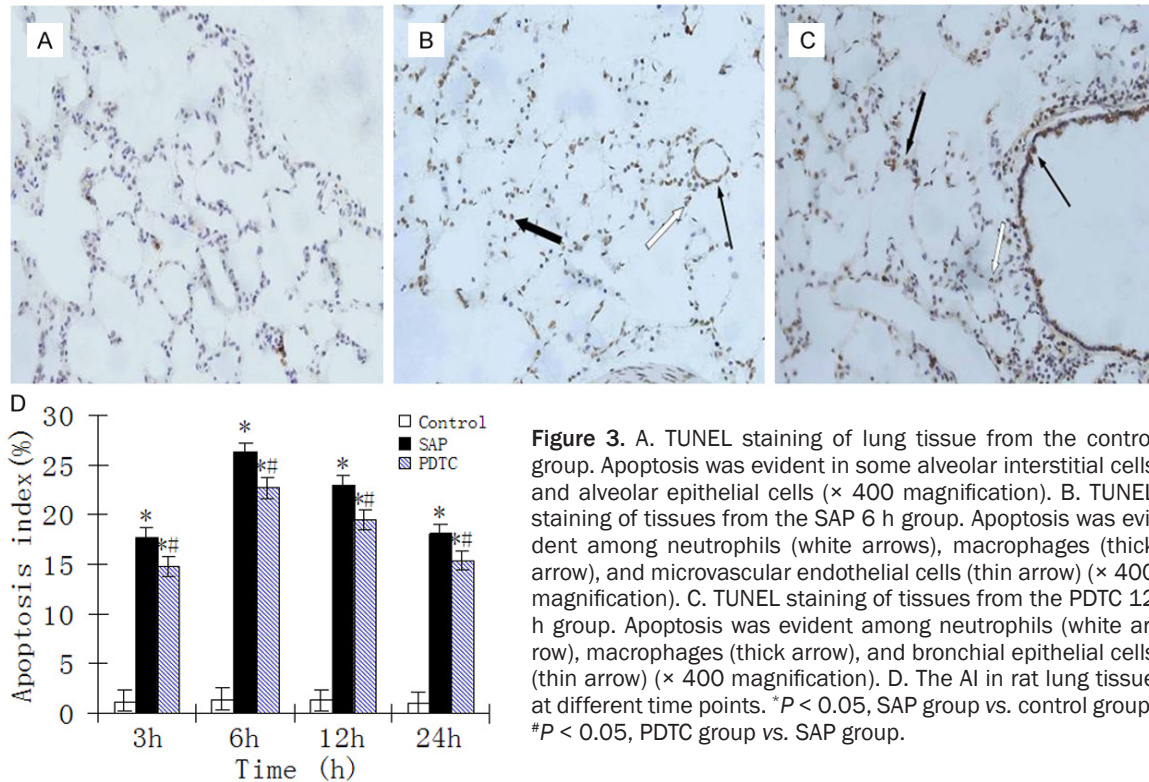


Figure 3. A. TUNEL staining of lung tissue from the control group. Apoptosis was evident in some alveolar interstitial cells and alveolar epithelial cells ($\times 400$ magnification). B. TUNEL staining of tissues from the SAP 6 h group. Apoptosis was evident among neutrophils (white arrows), macrophages (thick arrow), and microvascular endothelial cells (thin arrow) ($\times 400$ magnification). C. TUNEL staining of tissues from the PDTC 12 h group. Apoptosis was evident among neutrophils (white arrow), macrophages (thick arrow), and bronchial epithelial cells (thin arrow) ($\times 400$ magnification). D. The AI in rat lung tissue at different time points. *P < 0.05, SAP group vs. control group; #P < 0.05, PDTC group vs. SAP group.

group, with alveolar and interstitial edema, exudation of erythrocytes, and infiltration of inflammatory cells seen. Atelectasis of the local lobule was noticed as time progressed (**Figure 2F-H**). The histological abnormalities seen in PDTC rats were similar to those seen in SAP rats; however, exudation of erythrocytes and infiltration of inflammatory cells were ameliorated.

TEM analysis

The basic structure of alveolar epithelial cells and endothelial cells was normal for the control group (**Figure 2I**). The number of microvilli and osmiophilic lamellar bodies in type II alveolar

epithelial cells was reduced in SAP rats at 3 h. Vascular endothelial cells were swollen, basement membranes had widened, and nuclear chromatin had aggregated to the border of the nucleus. After 6 h, a thin layer of collagen between alveolar epithelial and vascular epithelial cells was apparent, there was intercellular edema, mitochondria of type II epithelial cells were swollen, basement membranes were wide and irregular, the number of osmiophilic lamellar bodies was reduced, cavitation was seen, and chromatin had aggregated to the border of the nucleus (**Figure 2G**). For the 12 and 24-h groups, there was an obvious increase in collagen activity between alveolar epithelium and vascular epithelial cells. The microvilli of

Effects of PDTC on NF- κ B and apoptosis

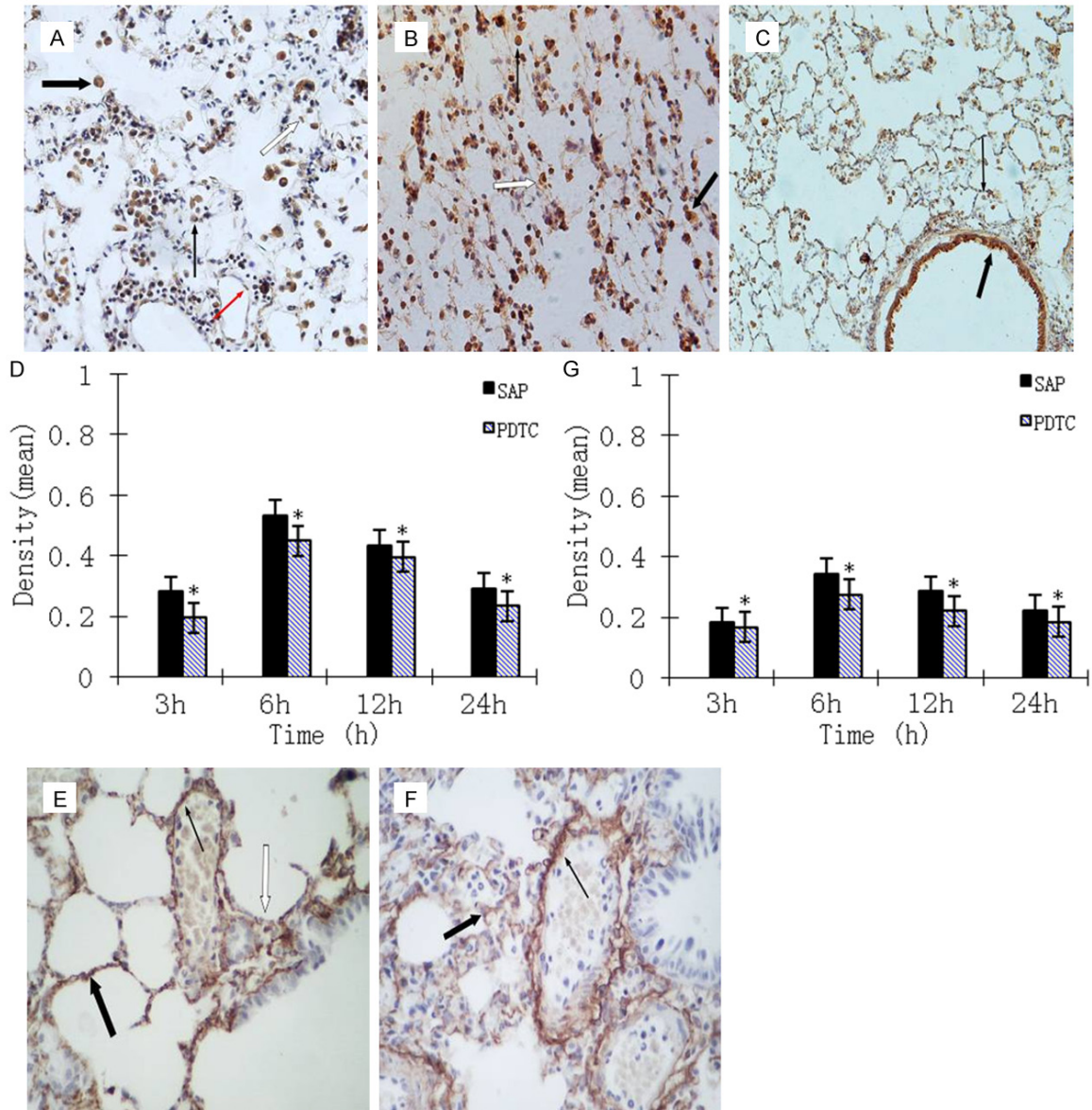


Figure 4. A. Immunohistochemical NF- κ B staining was mainly localized to neutrophils (thin black arrow), macrophages (thick black arrow), alveolar epithelial cells (white arrow) and microvascular endothelium cells (thin red arrow) in the SAP 6 h group ($\times 400$ magnification). B. Immunohistochemical staining of lung tissue from the PDTC 6 h group. Macrophages (thick arrow) and neutrophils (thin arrow) exhibited strong positive expression for NF- κ B with alveolar collapse (white arrow) seen ($\times 400$ magnification). C. Immunohistochemical staining of lung tissue from the SAP 6 h group. Macrophages (thin arrow) and bronchial epithelial cells (thick arrow) express NF- κ B ($\times 100$ magnification). D. Expression of NF- κ B in the lung tissue of rats at different time points. $*P < 0.05$, PDTC group vs. SAP group. E. Immunohistochemical staining of lung tissue from the SAP 6 h group. Fas staining was mainly localized in alveolar epithelial cells (thick arrow) and vascular endothelial cells (thin arrow), with alveolar collapse (white arrow) observed ($\times 400$ magnification). F. Immunohistochemical staining of lung tissue from the PDTC 24 h group. Alveolar epithelial cells (thick arrow) and vascular endothelial cells (thin arrow) express Fas ($\times 400$ magnification). G. Expression of Fas in the lung tissue of rats at different time points. $*P < 0.05$, PDTC group vs. SAP group.

the type II alveolar cell was significantly reduced and disordered. Osmiophilic lamellar bodies became loose, their numbers were decreased, cavitation was evident, and nuclei were concentrated and reduced in volume. Electron den-

sity was increased and mitochondria were swollen (**Figure 2K**). In vascular endothelial cells, mitochondria were swollen, basement membranes were wide, there was evidence of nuclear chromatin condensation, electron density

Effects of PDTC on NF-κB and apoptosis

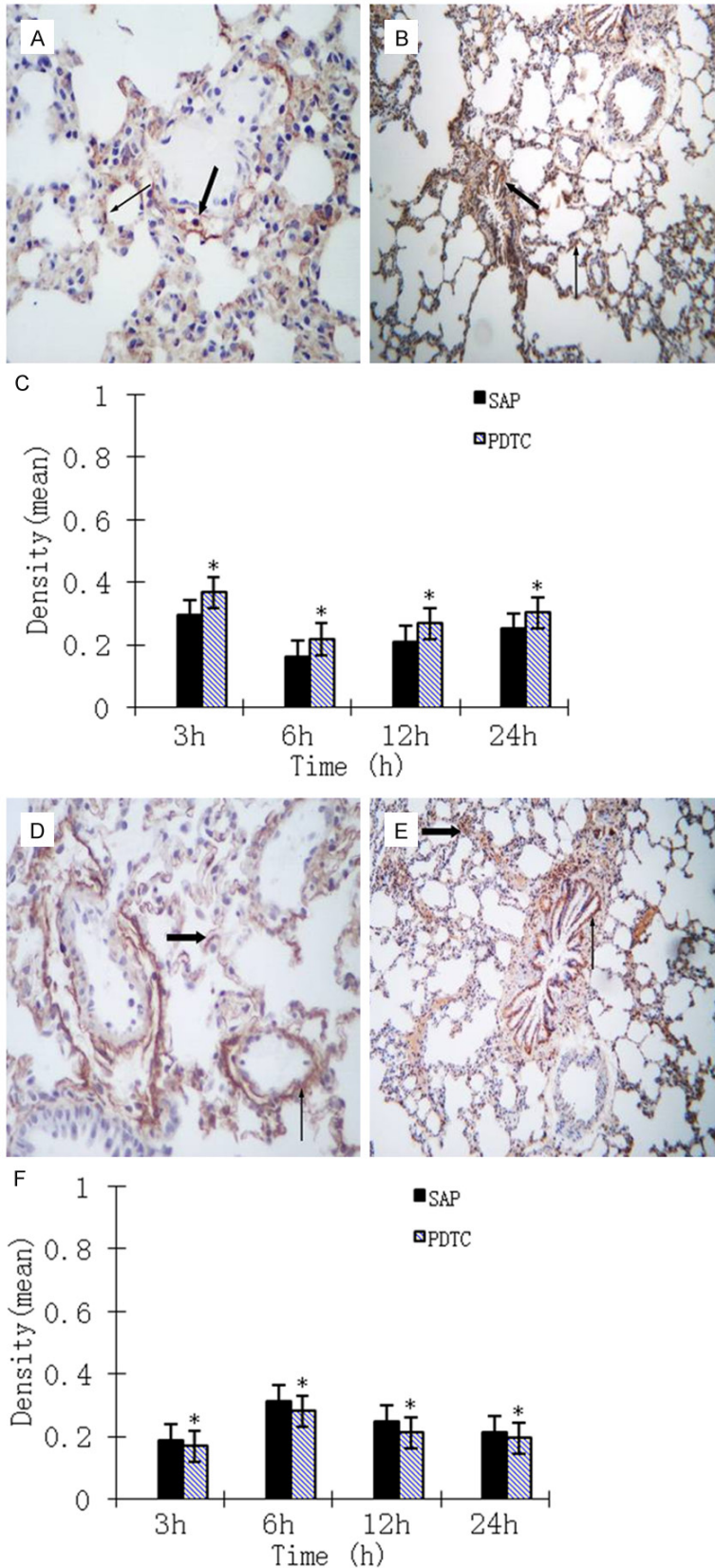


Figure 5. A. Bcl2 immunohistochemical staining of lung tissue from the SAP 12 h group. Bcl2 was

mainly localized to alveolar epithelial cells (thick arrow) and vascular endothelial cells (thin arrow) ($\times 400$ magnification). B. Bcl2 immunohistochemical staining of lung tissue from the PDTC 24 h group. Bronchial mucosa epithelial cells (thick arrow) and alveolar epithelial cells (thin arrow) express Bcl2 ($\times 100$ magnification). C. Expression of Bcl-2 in the lung tissue of rats at different time points. $*P < 0.05$, PDTC group vs. SAP group. D. TNF- α immunohistochemical staining of lung tissue from the SAP 6 h group. Alveolar epithelial cells (thick arrow) and vascular endothelial cells (thin arrow) are positive for TNF- α expression ($\times 400$ magnification). E. TNF- α immunohistochemical staining of lung tissue from the PDTC 12 h group. Alveolar epithelial cells (thick arrow) and bronchial mucosa epithelial cells (thin arrow) are positive for TNF- α expression ($\times 400$ magnification). F. Expression of TNF- α in the lung tissue of rats at different time points. $*P < 0.05$, PDTC group vs. SAP group.

was increased, the number of pinocytotic vesicles was increased and the respiratory membrane was thin. Compared with rats in the corresponding SAP group, PDTC rats were reduced in varying degrees (**Figure 2L**).

Cell apoptosis in pulmonary tissues

In control rats, only a small number of apoptotic cells were seen among epithelial and interstitial cells of the lung (**Figure 3A**). Apoptosis of neutrophils, monocytes/macrophages, bronchial epithelial cells, alveolar epithelial cells and some vascular endothelial cells was observed in SAP and PDTC rats. The AI at 3 h was significantly increased,

peaking at 6 h, then declined but was still at high levels at 24 h (**Figure 3B and 3C**). The AI

Effects of PDTC on NF- κ B and apoptosis

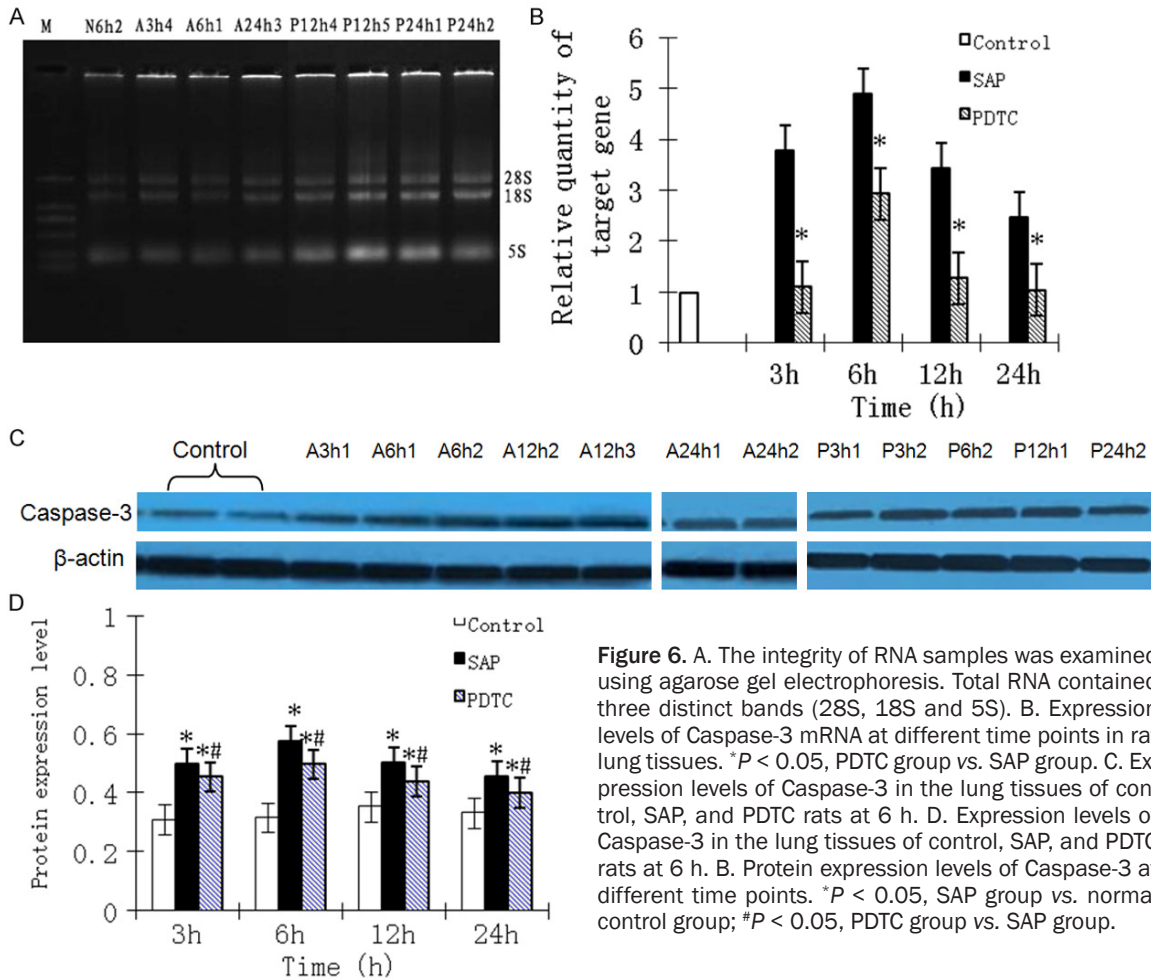


Figure 6. A. The integrity of RNA samples was examined using agarose gel electrophoresis. Total RNA contained three distinct bands (28S, 18S and 5S). B. Expression levels of Caspase-3 mRNA at different time points in rat lung tissues. * $P < 0.05$, PDTC group vs. SAP group. C. Expression levels of Caspase-3 in the lung tissues of control, SAP, and PDTC rats at 6 h. D. Expression levels of Caspase-3 in the lung tissues of control, SAP, and PDTC rats at 6 h. B. Protein expression levels of Caspase-3 at different time points. * $P < 0.05$, SAP group vs. normal control group; # $P < 0.05$, PDTC group vs. SAP group.

for all PDTC rats was lower compared with those in the SAP group ($P < 0.05$; **Figure 3D**).

NF- κ B, Fas, Bcl-2 and TNF- α expression in lung tissue

We observed NF- κ B expression in the neutrophils, macrophages, bronchial epithelial cells, alveolar epithelial cells and microvascular endothelium cells of SAP and PDTC rats. Expression of NF- κ B altered with the development of SAP, peaking at 6 h. Levels of NF- κ B then declined but were still significantly increased at 24 h. Expression levels of NF- κ B in all PDTC rats were lower compared with those in SAP rats ($P < 0.05$), but still higher than those in control rats ($P < 0.01$; **Figure 4A-D**). Fas expression was not evident in control rats. Expression of Fas in the lungs was significantly higher in PDTC rats than in control rats at all time points ($P < 0.01$) and was lower than that in SAP rats ($P < 0.05$). The expression of Fas and NF- κ B also appeared to be time dependent

(**Figure 4E-G**). We did not observe many Bcl-2-positive cells in control rats. Expression of Bcl-2 was seen in SAP and PDTC rats at each time point, with expression levels in PDTC rats significantly higher than those in SAP rats at all time points ($P < 0.05$). Positive signals were mainly located in the cytoplasm of bronchial epithelial, alveolar epithelial, and vascular endothelial cells. Expression of Bcl-2 decreased gradually as time progressed (**Figure 5A-C**). The expression pattern for TNF- α was similar to that for NF- κ B and Fas, peaking at 6 h, then declining but remaining high at 12 h. The expression levels of NF- κ B in all PDTC rats were lower compared with those in SAP rats ($P < 0.05$; **Figure 5D-F**).

Caspase-3 mRNA expression

Integrity of RNA for each sample was determined using agarose gel electrophoresis, with 28S, 18S and 5S bands clearly seen (Figure 6A). The $OD_{260}:OD_{280}$ ratio fluctuated between

1.8 and 2.0. Expression of caspase-3 mRNA in control rats was low. For SAP rats, caspase-3 mRNA expression was greatly increased at 3 h, peaking at 6 h, then decreasing but remaining high. In PDTC rats, expression of caspase-3 mRNA was increased at 3 h, peaking at 6 h, and then decreasing at 12 and 24 h. Expression of caspase-3 mRNA in PDTC rats was significantly lower than that in SAP rats ($P < 0.01$; **Figure 6B**).

Caspase-3 protein expression

Western blot analysis showed that caspase-3 protein expression was evident in all rats (**Figure 6C**). Compared with control rats, protein expression levels for caspase-3 were significantly higher in SAP and PDTC rats at each time point ($P < 0.01$). Following treatment with PDTC, caspase-3 levels were significantly decreased at each time point ($P < 0.05$). For SAP and PDTC rats, expression of caspase-3 was increased at 3 h, peaking at 6 h, then decreasing but staying at a high level at 24 h (**Figure 6D**).

Discussion

An imbalance in the cytokine network occurs during SAP, with pro-inflammatory cytokines TNF- α and IL-1 present at much higher levels than anti-inflammatory cytokines such as IL-2, IL-10 and IL-12. NF- κ B participates in the transcription of various inflammatory mediator genes [19]. In the current study, during the early stages of SAP, obvious expression of NF- κ B was observed. Its expression decreased after an initial rise and then increased again; peak expression was seen at 6 h. NF- κ B in the lung was mainly expressed in neutrophils, mononuclear macrophages, bronchial epithelial cells, alveolar epithelial cells, and some microvascular endothelial cells. Positive signals were seen in the cytoplasm and nucleus of positive cells, with a correlation between NF- κ B expression and pathological changes in lung tissues. This confirms that NF- κ B participates in the progress of pulmonary injury, which is complicated by SAP during the early stages. Serum amylase and lipase levels are indicative of pancreatitis [20]. Changes in the concentration of serum amylase and lipase were consistent with pathological changes in pancreas and lung tissues. We observed some correlation between the expression of NF- κ B in the lung tissues of rats

with SAP and the concentration of serum amylase and lipase. These findings suggest that, as a direct Griggling factor of SAP, pancreatin might directly damage pancreatic tissues, thereby leading to multiple organ failure through inflammatory reactions activated and mediated by NF- κ B.

Apoptosis is an active energy-intensive process regulated by a variety of apoptosis-related genes and it differs from necrosis. There are three main pathways that lead to the induction of apoptosis: the mitochondrial pathway; the death receptor pathway; and the endoplasmic reticulum pathway [21]. Recent studies have shown that NF- κ B has a close association with apoptosis, and is involved in the transcriptional regulation of various apoptosis-related genes [22, 23]. Yet the specific mechanisms involved remain to be elucidated. Some studies have also shown that the death of pancreatic cells involves a form of apoptosis during acute pancreatitis; there was a negative correlation between severity of acute pancreatitis and rate of apoptosis for pancreatic cells [24]. Subsequent studies [25, 26] have indicated that induction of pancreatic acinar cell apoptosis by different methods can relieve AP conditions. However, a relationship between NF- κ B and apoptosis in lung cells during pulmonary injury in conjunction with SAP has not been reported. We observed that during pulmonary injury complicated with SAP, apoptotic cells in the lung were present in greater numbers compared with those in the control group and had some correlation with pulmonary injury. The AI in cells of lung tissues showed time-dependent and dynamic changes. Meanwhile, the degree of apoptosis in lung tissues was consistent with pathological changes, suggesting that apoptosis in lung tissues not only participated in the early pathological process of pancreatitis-associated lung injury (PALI), but was also associated with its progression. There was a correlation between NF- κ B expression and apoptosis in lung tissues, except at 24 h, suggesting an intrinsic link between NF- κ B activation and apoptosis in lung tissues. However, the exact mechanisms involved remain to be identified.

Apoptosis plays an important role in the onset, progression and prognosis of SAP. TNF- α is a pro-inflammatory cytokine that can stimulate the acute phase reaction, and is a major player during the cascade of cytokine release. The

TNF- α receptors (TNFRs) are known as death receptors and can induce apoptosis [27]. Fas belongs to the TNFR family; it is a type I transmembrane protein and the receptor for Fas L. It can induce Fas expression in apoptotic cells when it binds to Fas L or Fas antibody; it is a major inducer of apoptosis [28]. The Fas/Fas L apoptosis pathway mediates the apoptosis of acinar cells in acute pancreatitis. Deletion of the Fas gene can aggravate acute pancreatitis in rat models induced by cerulein [29]. The Fas protein has been confirmed as an important cell death factor; it is expressed in different tissues and mediates cell death through the activation of caspase-3. Bcl-2 is a member of the Bcl-2 family of apoptosis control genes and is an inhibitor of apoptosis. Bcl-2 resides in the nuclear and endoplasmic reticulum membranes, along with external and internal membranes of mitochondria [30]. Bcl-2 can form heterodimers by binding to the apoptosis-promoting gene Bax. This can lead to increased permeability of the outer mitochondrial membrane and induction of apoptosis [31]. Because the Bcl-2 family controls the permeability of the inner and outer mitochondrial membranes, it is the main regulator of the mitochondrial apoptosis pathway through a series of downstream genes that play a role in regulating apoptosis [32]. Activation of caspase family members occurs during apoptosis, with Caspase-3 a key regulator of the entire apoptotic cascade [33, 34].

We found that expression levels of Fas, TNF- α , and caspase-3 mRNAs, along with the caspase-3 protein, first increased, peaking at 6 h, and then decreased. This was consistent with the changes in the AI. However, the expression pattern for Bcl-2 exhibited the opposite pattern, suggesting that apoptosis pathways mediated by Fas, TNF- α , Bcl-2 and Caspase-3 are involved in apoptosis in lung tissue during SAP. These apoptosis pathways include at least one death receptor pathway and a mitochondrial pathway. Despite the presence of factors inhibiting apoptosis, rates of apoptosis tended to increase. This finding indicated that different apoptotic pathways are not fully independent, and in some cases there is cross-talk between pathways. At the same time, there were changes in the expression patterns for Fas, TNF- α , Bcl-2, Caspase-3 mRNAs and the Caspase-3 protein that were consistent with the expression of NF- κ B. These observations showed that

NF- κ B, as a nuclear transcription factor, mediated the expression of apoptosis-regulating genes such as Fas, TNF- α and Bcl-2. We postulate, from our results, that NF- κ B is activated in lung tissue during SAP and combines with the κ B site of intracellular apoptosis-regulating genes, thereby mediating the expression of apoptosis-regulating genes. This then initiates the various apoptosis pathways, which in turn initiates caspase cascade reactions. However, the detailed mechanisms involved require further investigation.

Given that NF- κ B participates in severe acute pancreatitis associated with lung injury, reducing its activity or preventing its activation would help reduce the severity of ALI. PDTC is a selective NF- κ B inhibitor and antioxidant. To date, all irritants capable of inducing NF- κ B can be blocked by antioxidants. This reduces its ability to bind to DNA, interferes with the signal path of activation for NF- κ B, and stabilizes or increases the synthesis mechanism of I κ B α to inhibit NF- κ B activity [35]. A SAP rat model was pretreated with PDTC and compared with SAP and control rats. Results showed that pathological changes were improved after the application of PDTC. The concentration of serum amylase and lipase was significantly reduced, suggesting that PDTC could relieve symptoms of pulmonary injury complicated with SAP, consistent with clinical reports. Following the application of PDTC, the optical density average of NF- κ B was significantly reduced. Electron microscopy results showed that PDTC could relieve the injuries of lung tissue cells to varying extents. It could be inferred that PDTC indirectly inhibits the activation of NF- κ B by inhibiting oxidative phosphorylation of I κ B. After application of PDTC, the number of apoptotic cells in the lung was low, expression of pro-apoptosis factors was increased, expression of anti-apoptosis factors was decreased, and the apoptosis protease cascade reduced. The mechanisms involved remain unclear; they could be related to inhibition of NF- κ B activity, but further study is needed to clarify this.

In conclusion, NF- κ B plays a key role over the course of pulmonary injury complicated with SAP, and in the induction of apoptosis in the lungs. Its activation is a pathway for a variety of inflammatory reactions. Activated NF- κ B also causes apoptosis of lung tissue by regulating the expression of genes related to cell death.

This ultimately leads to pulmonary injuries, including pulmonary vascular endothelial cell injury. It is important that further study into the correlation and mechanisms between NF- κ B activation and apoptosis in the lungs during pulmonary injury complicated with SAP is carried out. It remains to be seen how to selectively inhibit the activation of NF- κ B and specifically reduce the expression of pro-inflammatory genes, thereby decreasing inflammatory cytokine levels. Developing these therapeutic strategies should help reduce the complications and mortality associated with SAP.

Disclosure of conflict of interest

None.

Address correspondence to: Huijun Yang, Department of Human Anatomy, West China School of Preclinical and Forensic Medicine, Sichuan University, No. 17 Renmin South Road, Chengdu 610041, China. Tel: +86 13980034804; E-mail: he500209@163.com

References

- [1] Algül H, Treiber M, Lesina M, Nakhai H, Saur D, Geisler F, Pfeifer A, Paxian S, Schmid RM. Pancreas-specific RelA/p65 truncation increases susceptibility of acini to inflammation-associated cell death following cerulein pancreatitis. *J Clin Invest* 2007; 117: 1490-1501.
- [2] Giakoustidis A, Mudan SS, Giakoustidis D. Dissecting the stress activating signaling pathways in acute pancreatitis. *Hepatogastroenterology* 2010; 57: 653-656.
- [3] Surbatović M, Jovanović K, Radaković S, Filipović N. Pathophysiological aspects of severe acute pancreatitis-associated lung injury. *Srp Arh Celok Lek* 2005; 133: 76-81.
- [4] Pandol SJ, Saluja AK, Imrie CW, Banks PA. Acute pancreatitis: bench to the bedside. *Gastroenterology* 2007; 132: 1127-1151.
- [5] Sehnert B, Burkhardt H, Wessels JT, Schröder A, May MJ, Vestweber D, Zwerina J, Warnatz K, Nimmerjahn F, Schett G, Dübel S, Voll RE. NF- κ B inhibitor targeted to activated endothelium demonstrates a critical role of endothelial NF- κ B in immune-mediated diseases. *Proc Natl Acad Sci U S A* 2013; 110: 16556-16561.
- [6] Kan SH, Hang F, Tang J, Gao Y, Yu CL. Role of Intrapulmonary Expression of Inducible Nitric Oxide Synthase Gene and Nuclear Factor kappaB Activation in Severe Pancreatitis-associated Lung Injury. *Inflammation* 2010; 33: 287-294.
- [7] Zhang JJ, Xu ZM, Chang H, Zhang CM, Dai HY, Ji XQ, Li C, Wang XF. Pyrrolidine dithiocarbamate attenuates nuclear factor- κ B activation, cyclooxygenase-2 expression and prostaglandin E2 production in human endometriotic epithelial cells. *Gynecol Obstet Invest* 2011; 72: 163-168.
- [8] Luo JL, Kamata H, Karin M. The anti-death machinery in IKK/NF-kappaB signaling. *J Clin Immunol* 2005; 25: 541-550.
- [9] Zheng Y, Ouaaz F, Bruzzo P, Singh V, Gerondakis S, Beg AA. NF- κ B RelA (p65) is essential for TNF- α -induced Fas expression but dispensable for both TCR-induced expression and activation-induced cell death. *Immunol* 2001; 166: 4949-4957.
- [10] Alvira CM. Nuclear factor-kappa-B signaling in lung development and disease: One pathway, numerous functions. *Birth Defects Res A Clin Mol Teratol* 2014; 100: 202-216.
- [11] Nikolettou V, Markaki M, Palikaras K, Tavernarakis N. Crosstalk between apoptosis, necrosis and autophagy. *Biochim Biophys Acta* 2013; 1833: 3448-3459.
- [12] Beug ST, Cheung HH, LaCasse EC, Korneluk RG. Modulation of immune signalling by inhibitors of apoptosis. *Trends Immunol* 2012; 33: 535-545.
- [13] Fauvet R, Dufournet C, Poncelet C, Uzan C, Hugol D, Daraï E. Expression of pro-apoptotic (p53, p21, bax, bak and fas) and anti-apoptotic (bcl-2 and bcl-x) proteins in serous versus mucinous borderline ovarian tumours. *J Surg Oncol* 2005; 92: 337-343.
- [14] Gómez-Navarro J, Arafat W, Xiang J. Gene therapy for carcinoma of the breast: Pro-apoptotic gene therapy. *Breast Cancer Res* 2000; 2: 32-44.
- [15] Chen QY, Lu GH, Wu YQ, Zheng Y, Xu K, Wu LJ, Jiang ZY, Feng R, Zhou JY. Curcumin induces mitochondria pathway mediated cell apoptosis in A549 lung adenocarcinoma cells. *Oncol Rep* 2010; 23: 1285-1292.
- [16] Gougeon ML, Kroemer G. Charming to death: caspase-dependent or -independent? *Cell Death Differ* 2003; 10: 390-392.
- [17] Aho HJ, Nevalainen TJ. Experimental pancreatitis in the rat. Ultrastructure of sodium taurocholate-induced pancreatic lesions. *Scand J Gastroenterol* 1980; 15: 417-424.
- [18] Schmittgen TD, Livak KJ. Analyzing real-time PCR data by the comparative C(T) method. *Nat Protoc* 2008; 3: 1101-1108.
- [19] Rakonczay Z Jr, Hegyi P, Takács T, McCarroll J, Saluja AK. The role of NF-kappaB activation in the pathogenesis of acute pancreatitis. *Gut* 2008; 57: 259-267.
- [20] Walgren JL, Mitchell MD, Whiteley LO, Thompson DC. Evaluation of two novel peptide safety

Effects of PDTC on NF- κ B and apoptosis

- markers for exocrine pancreatic toxicity. *Toxicol Sci* 2007; 96: 184-193.
- [21] Muñoz-Pinedo C. Signaling pathways that regulate life and cell death: evolution of apoptosis in the context of self-defense. *Adv Exp Med Biol* 2012; 738: 124-143
- [22] Rawat N, Alhamdani A, McAdam E, Cronin J, Eltahir Z, Lewis P, Griffiths P, Baxter JN, Jenkins GJ. Curcumin abrogates bile-induced NF- κ B activity and DNA damage in vitro and suppresses NF- κ B activity whilst promoting apoptosis in vivo, suggesting chemopreventative potential in Barrett's oesophagus. *Clin Transl Oncol* 2012; 14: 302-311.
- [23] Chen X, Kandasamy K, Srivastava RK. Differential roles of RelA(p65) and c-Rel subunits of nuclear factor kappa B in tumor necrosis factor-related apoptosis-inducing ligand signaling. *Cancer Res* 2003; 63: 1059-1066.
- [24] Zhang XP, Tian H, Lu B, Chen L, Xu RJ, Wang KY, Wang ZW, Cheng QH, Shen HP. Tissue microarrays in pathological examination of apoptotic acinar cells induced by dexamethasone in the pancreas of rats with severe acute pancreatitis. *Hepatobiliary Pancreat Dis Int* 2007; 6: 527-536.
- [25] Zhao M, Xue DB, Zheng B, Zhang WH, Pan SH, Sun B. Induction of apoptosis by artemisinin relieving the severity of inflammation in caerulein-induced acute pancreatitis. *World J Gastroenterol* 2007; 13: 5612-5617.
- [26] Booth DM, Murphy JA, Mukherjee R, Awais M, Neoptolemos JP, Gerasimenko OV, Tepikin AV, Petersen OH, Sutton R, Criddle DN. Reactive oxygen species induced by bile acid induce apoptosis and protect against necrosis in pancreatic acinar cells. *Gastroenterology* 2011; 140: 2116-2125.
- [27] Malleo G, Mazzon E, Genovese T, Di Paola R, Muià C, Centorrino T, Siritwardena AK, Cuzzocrea S. Etanercept attenuates the development of cerulein-induced acute pancreatitis in mice: a comparison with TNF-alpha genetic deletion. *Shock* 2007; 27: 542-551.
- [28] Keller ET, Liu Q, Zhou Q, Zhang J. Targeting the Notch signaling pathway in cancer therapeutics. *Thoracic Cancer* 2014; 5: 473-486.
- [29] Jeyarajah DR, Kielar M, Gokaslan ST, Lindberg G, Lu CY. Fas deficiency exacerbates cerulein-induced pancreatitis. *J Invest Surg* 2003; 16: 325-333.
- [30] Saxena N, Katiyar SP, Liu Y, Grover A, Gao R, Sundar D, Kaul SC, Wadhwa R. Molecular interactions of Bcl-2 and Bcl-xL with mortalin: identification and functional characterization. *Biosci Rep* 2013; 33.
- [31] Harris MH, Thompson CB. The role of the Bcl-2 family in the regulation of outer mitochondrial membrane permeability. *Cell Death Differ* 2000; 7: 1182-1191.
- [32] Tsukahara S, Yamamoto S, Tin-Tin-Win-Shwe, Ahmed S, Kunugita N, Arashidani K, Fujimaki H.. Inhalation of low-level formaldehyde increases the Bcl-2/Bax expression ratio in the hippocampus of immunologically sensitized mice. *Neuroimmunomodulation* 2006; 13: 63-68.
- [33] Snigdha S, Smith ED, Prieto GA, Cotman CW. Caspase-3 activation as a bifurcation point between plasticity and cell death. *Neurosci Bull* 2012; 28: 14-24.
- [34] Okazaki S, Ogawa F, Iwata Y, Hara T, Muroi E, Komura K, Takenaka M, Shimizu K, Hasegawa M, Fujimoto M, Sato S. Autoantibody against caspase-3, an executioner of apoptosis, in patients with systemic sclerosis. *Rheumatol Int* 2010; 30: 871-878.
- [35] Yang S, Bing M, Chen F, Sun Y, Chen H, Chen W. Autophagy regulation by the nuclear factor κ B signal axis in acute pancreatitis. *Pancreas* 2012; 41: 367-373.